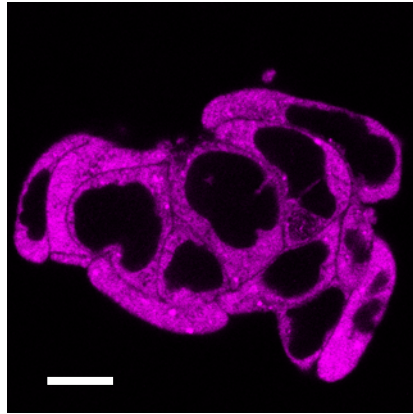
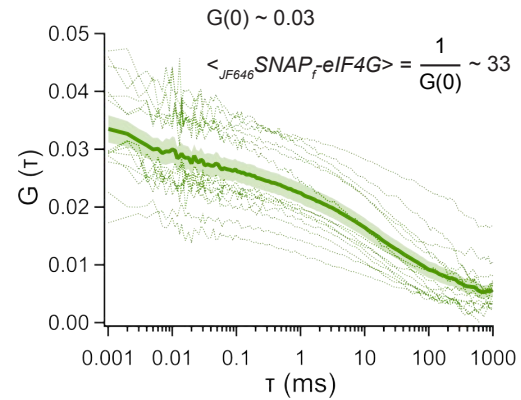
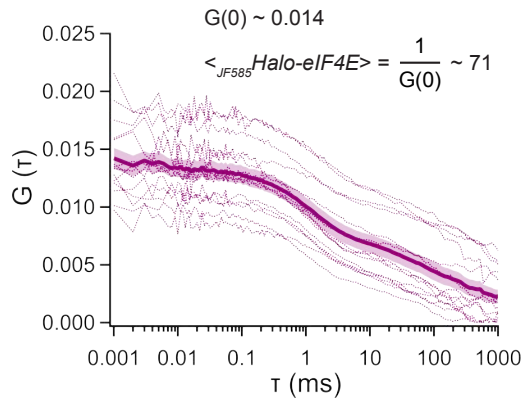
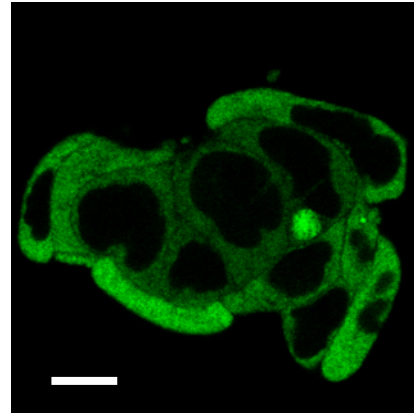
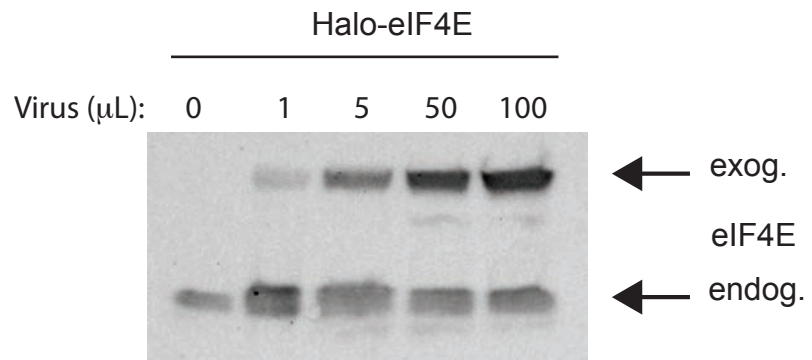


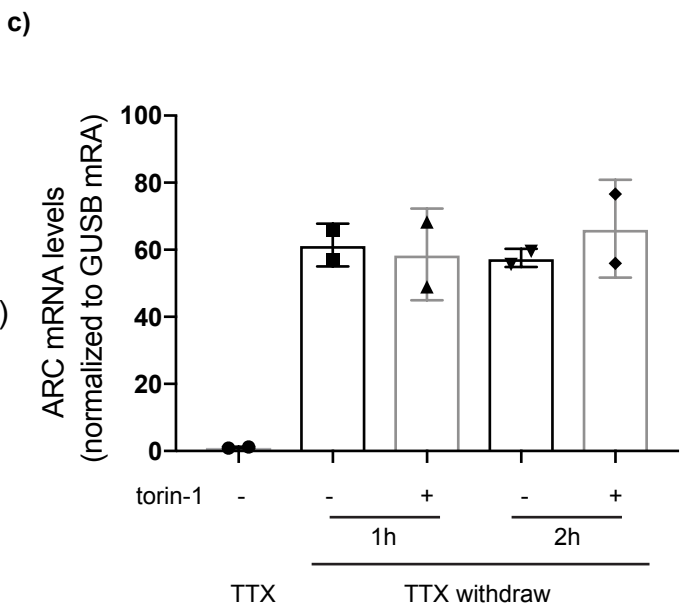
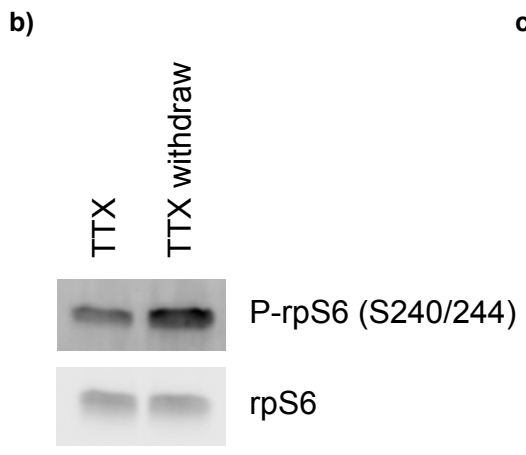
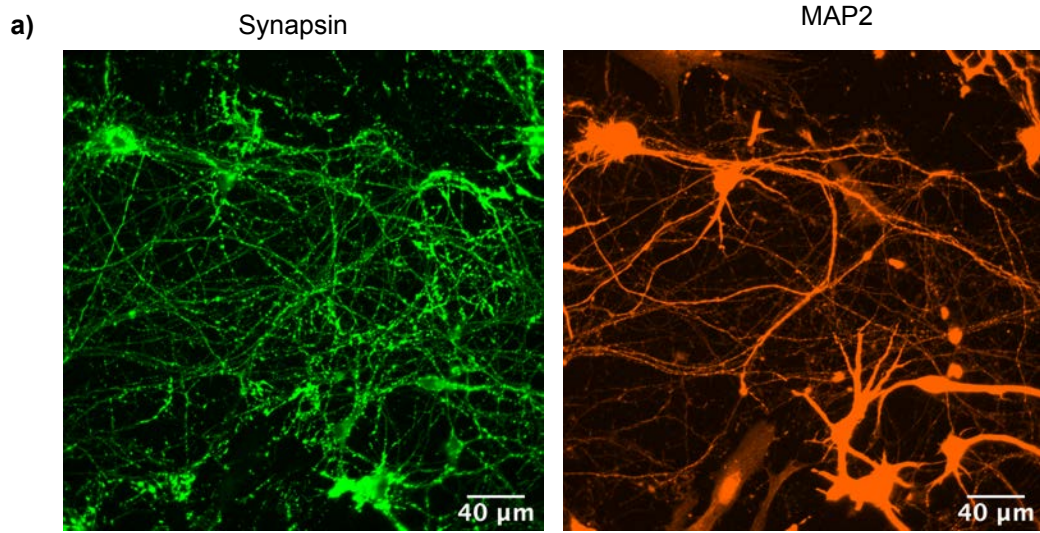
JF585 Halo-eIF4E



JF646 SNAP_f-eIF4G







Statistical Analysis

for Fig 4g:

Student t-test: two mean values of two distributions:

alpha = 0.001:

Sample 1: eiF4E
Number of Points=355730
Mean=0.4932
Stdv=0.309552
Degrees of Freedom=355729

Sample 2: eiF4G
Number of Points=462072
Mean=0.337417
Stdv=0.231293
Degrees of Freedom=462071

Combined effective degrees of freedom: 636684

T-Test Statistic: 251.021

Lower Critical Value: -3.29054

Upper Critical Value: 3.29054

HO: avg1=avg2 HO Acceptance range (0.0005,0.9995) ==> **H0 Rejected**

C.I. mean1=[0.493197,0.493203] C.I. mean2=[0.337415,0.337419]

alpha = 0.001:

Sample 1: eiF4E
Number of Points=355730
Mean=0.4932
Stdv=0.309552
Degrees of Freedom=355729

Sample 2: comoving eiF4E/eiF4G
Number of Points=7947
Mean=0.318147
Stdv=0.601916
Degrees of Freedom=7946

Combined effective degrees of freedom: 8040.17

T-Test Statistic: 25.8498

Lower Critical Value: -3.29174

Upper Critical Value: 3.29174

HO: avg1=avg2 HO Acceptance range (0.0005,0.9995) ==> **H0 Rejected**

C.I. mean1=[0.493197,0.493203] C.I. mean2=[0.317897,0.318396]

alpha = 0.01:

Sample 1: eiF4G
Number of Points=462072
Mean=0.337417
Stdv=0.231293
Degrees of Freedom=462071

Sample 2: comoving eiF4E/eiF4G
Number of Points=7947
Mean=0.318147
Stdv=0.601916
Degrees of Freedom=7946

Combined effective degrees of freedom: 7986.41

T-Test Statistic: 2.85038

Lower Critical Value: -2.57645

Upper Critical Value: 2.57645

HO: avg1=avg2 HO Acceptance range (0.005,0.995) ==> **H0 Rejected**

C.I. mean1=[0.337416,0.337418] C.I. mean2=[0.317951,0.318342]

for Fig 6a:

Student t-test: two mean values of two distributions:

alpha = 0.001:

Sample 1: eiF4E
Number of Points=252266
Mean=0.781231
Stdv=0.742717
Degrees of Freedom=252265

Sample 2: eiF4G
Number of Points=318077
Mean=0.474816
Stdv=0.637885
Degrees of Freedom=318076

Combined effective degrees of freedom: 498459

T-Test Statistic: 164.589

Lower Critical Value: -3.29055

Upper Critical Value: 3.29055

HO: avg1=avg2 HO Acceptance range (0.0005,0.9995) ==> **H0 Rejected**

C.I. mean1=[0.781222,0.781241] C.I. mean2=[0.47481,0.474823]

Supplementary Figure Legends

Supplementary Fig. 1 Halo-eIF4E rescue cell proliferation and binds the 5'cap mRNA.

a) Vector control or Halo-eIF4E expressed in NIH3T3 cells. Total cell lysates were analyzed by western blotting with eIF4E and Halo-tag antibodies. No degradation products were detected. **b)** Vector control or Halo-eIF4E expressed in NIH3T3 cells infected with scrambled shRNA control (Scrambled) or shRNA targeting eIF4E (shRNA eIF4E). Total cell lysates were analyzed by western blotting. eIF4E antibodies detect both endogenous and exogenous eIF4E as indicated by the arrows. GAPDH was used as loading control. **c)** Cells described in a) were treated with DMSO (vehicle) or torin-1 for 1 hour. Total cell lysates (Input) were subjected to m7GTP-pull down assay and analyzed with the indicated antibodies. The Halo tag does not prevent eIF4E binding to the 5'cap analogue or 4E-BP1 binding upon mTOR inhibition. **d)** Proliferation of the indicated cells was measured by 5-bromo-2'-deoxyuridine (BrdU) incorporation. The results are represented as mean absorbance at 370 nm \pm s.d. from three independent experiments

Supplementary Fig. 2 Slow diffusion of Halo-eIF4 in the cytoplasm of translating cells detected by FCS.

NIH3T3 cells that express Halo-eIF4E, in which the endogenous counterpart was knocked down by shRNA, were treated with DMSO (control) or 250nM torin-1 for 2 hours and subjected to FCS. **a,b)** Representative examples of J_{F646} Halo-eIF4E fluorescent fluctuations throughout the focal volume, in the cytoplasm and in the nucleus and in the indicated conditions. Major fluctuations (see within rectangle for representative example) are only detected in the cytoplasm of translating cells. **c,d)** Individual autocorrelations (in red) of the averaged autocorrelations (in black) depicting the temporal diffusion of eIF4E in the cytoplasm (left panel) and nucleus (right panel).

Supplementary Fig. 3 Overexpression SNAPf-4E-BP1 slowed down cell proliferation and increased torin-1 efficacy.

a) Vector control or SNAPf-4E-BP1 were expressed in NIH3T3 cells infected with scrambled shRNA control (Scrambled) or shRNA targeting 4EBP1 (sh4EBP1). Total cell lysates were analyzed by western blotting. 4E-BP1 antibodies detect both endogenous and exogenous 4E-BP1 as indicated by the arrows. **b)** Proliferation of NIH3T3 cells infected with scrambled shRNA control (Scrambled) or shRNA targeting endogenous 4EBP1 (sh4EBP1) that express Vector control or SNAPf-4E-BP1 was measured by 5-bromo-2'-deoxyuridine (BrdU) incorporation. The results are represented as mean absorbance at 370 nm \pm s.d. from three independent experiments. SNAPf-4E-BP1 overexpression slightly decreased cell proliferation at 48 and 72 hours. **c)** Cells described in a) were treated with vehicle control (DMSO) or 250nM torin-1 for 16 hours. Proliferation was measured as in b). The results are represented as mean absorbance at 370 nm \pm s.d. from three independent experiments. 4E-BP1 overexpression increase the cytostatic effect of torin-1.

Supplementary Fig. 4 eIF4E:4E-BP1 complexes accumulate in the nucleus upon prolonged mTOR inhibition.

a-c) Differentiated mESC in which Halo and SNAPf tag were inserted into the Eif4e and Eif4ebp1 locus, respectively, were treated with vehicle (DMSO) or 250nM torin-1 from 2 to 3 hours. Halo-eIF4E and Snapf-4E-BP1 autocorrelations diffuse as fast as the nuclear counterparts in the indicated conditions (a). Data are presented as a mean value \pm SEM. Representative field of view of differentiated mESC showing subcellular distribution of $JF585$ Halo-eIF4E and $JF646$ Snapf-4E-BP1 in control and torin-1 treated cells. Images depicted distribution of initiation factors in living cells (b). eIF4E translocate to the nucleus 3 hours upon mTOR inhibition. Simultaneous diffusion of $JF585$ Halo-eIF4E and $JF646$ Snapf-4E-BP1 analyzed in differentiated mESC by fluorescent cross-correlation spectroscopy (FCCS) in the indicated conditions. Cross-correlation was detected in the cytoplasm and in the nucleus 3 hours upon mTOR inhibition. No cross-correlation was observed in the nucleus of translating cells (control). Data are presented as mean values \pm SEM (c).

Supplementary Fig. 5 Impaired translation initiation due to eIF4E release from the 5'cap with no major difference in global translation.

a,b) Differentiated mESC Halo-eIF4E^{+/+} (a) and NIH3T3 (b) that express exogenous Halo-eIF4E were treated with DMSO (control) or 250nM torin-1 for 2 hours. Cytosolic extracts were sedimented by centrifugation on 5-50% sucrose gradients. Free ribosomal subunits (40S and 60S), monosomes (80S) and translating ribosomes (polysome) are indicated. Increased in the 80S peak and decreased polysome levels showed initiation defects upon mTOR inhibition. Global protein synthesis measure by 35S-Met/Cys incorporation in the indicated cell lines treated with DMSO (-) or torin-1 (+) for 2 hours (c). 35S-Met/Cys incorporation was normalized by total proteins and expressed as arbitrary units (A.U). Each replicate is represented as a single point on the corresponding bar graph (n=3). Data are presented as a mean values \pm SD). Expression of Halo-eIF4E does not sensitize the cells to torin-1 treatment.

Supplementary Fig. 6 Tagging of endogenous translation factors does not affect mESC viability or their binding dynamics.

a) Halo-tag inserted in the endogenous locus of EIF4E by Crispr/cas9. Total cell lysates from parental, heterozygote and homozygote cells were analyzed by western blotting using eIF4E antibodies. β -actin was used as a loading control. Heterozygote (Halo-eIF4E^{+/-} or homozygote insertion (Halo-eIF4E^{+/+}) is shown. **b)** Proliferation of parental and Halo-eIF4E homozygote (Halo-eIF4E^{+/+}) differentiated to fibroblasts was measured by 5-bromo-2'-deoxyuridine (BrdU) incorporation. The results are represented as mean absorbance at 370 nm \pm s.d. from three independent experiments. **c)** SNAPf-tag was inserted in the endogenous locus of EIF4G1. Total cell lysates (input) from parental and eIF4G1 homozygote differentiated mESC (eIF4G1^{+/+}) were subjected to m7GTP-pull down assay and analyzed by western blotting using the indicated antibodies. **d,e)** Autocorrelation of endogenous $JF646$ Halo-eIF4E1 and $JF646$ SNAPf-eIF4G1 in cells described above. Data are presented as mean values \pm SEM). Cells were treated with DMSO (control) or 250nM torin-1 for 2 hours (2h). eIF4E and eIF4G1 molecules diffuse slower in the cytoplasmic of translating cells as compared to nuclear counterpart. Upon torin-1 treatment (torin-1 (2h)), cytoplasmic eIF4E molecules, but not eIF4G, diffuse as fast as the nuclear counterpart.

Supplementary Fig. 7 Measured apparent eIF4E and eIF4G concentrations in double knock-in Halo-eIF4E^{+/+}/SNAPf-eIF4G^{+/+} cells labeled with JF585Halo-eIF4E and JF646SNAPf-eIF4G.

(top) Representative field of view of double knock-in Halo-eIF4E^{+/+}/SNAP-eIF4G^{+/+} mESCs showing subcellular distribution of JF585Halo-eIF4E (in magenta) and JF646Snapf-eIF4G (in green). Images depicted distribution of initiation factors in living cells (scale bar: 10 μm). (bottom) Simultaneous diffusion of JF585Halo-eIF4E and JF646Snapf-eIF4G analyzed by FCS. Non-normalized autocorrelation curves representing individual diffusion of JF585Halo-eIF4E (in magenta) and JF646SNAPf-eIF4G (in green) in the indicated conditions (N=14±S.E.M.). The average number of molecules <N> in a focal volume was calculated from the G(0) timepoints of the non-normalized FCS curves. <N> was determined to be 71 for JF585Halo-eIF4E and 33 for JF646Snapf-eIF4G. The calculated apparent concentrations are 249 nM for JF585Halo-eIF4E and 113 nM for JF646Snapf-eIF4G. Values of <N> in the range between 0.1 and 100 are well suited for FCS (Ries et al. 2012; Hess et al. 2022).

Supplementary Fig. 8 Expression of Halo-eIF4E in primary cortical neurons.

Primary cortical neurons were infected with 1 μL, 5 μL, 50 μL and 100 μL of lentivirus carrying Halo-eIF4E (concentration at 2E⁷ IU/mL). Protein extracts were analyzed by western blotting using anti-eIF4E antibodies. Endogenous and exogenous eIF4E are indicated. Single-particle tracking was performed in neurons that express Halo-eIF4E at a similar level as the endogenous counterpart (5 μL) to minimize overexpression artefacts in the neuronal processes.

Supplementary Fig. 9 mTOR inhibition does not affect ARC mRNA stability.

a) Differentiated neurons derived from mESC. Immunostaining with the pre-synaptic marker Synapsin and the neuronal marker MAP2 is shown. **b)** Cells described in a) were treated for 16 hours with TTX. After 16 hours, TTX was removed for 2 hours and protein extracts were analyzed by western blot with the indicated antibodies. TTX withdraw increased mTOR activity. **c)** Neurons were activated by TTX withdrawal with and without 250nM torin-1 for 1 and 2 hours. Expression levels of the mature ARC mRNA, in the indicated conditions, were determined by RT-qPCR (n=3). Data are presented as mean values +/- SD). Values were normalized to the levels of the house-keeping GUSB mRNA.